ELSEVIER

NeuroImage

www.elsevier.com/locate/ynimg
NeuroImage 36 (2007) 606 – 616

Tractography-guided statistics (TGIS) in diffusion tensor imaging for the detection of gender difference of fiber integrity in the midsagittal and parasagittal corpora callosa

Jungsu S. Oh,[a,b,c] In Chan Song,[d,*] Jae Sung Lee,[a] Hyejin Kang,[a] Kwang Suk Park,[b] Eunjoo Kang,[e] and Dong Soo Lee[a]

[a]*Department of Nuclear Medicine, Seoul National University College of Medicine, Seoul, South Korea*
[b]*Department of Biomedical Engineering, Seoul National University College of Medicine, Seoul, South Korea*
[c]*Biomedical Engineering Branch, Division of Basic Science, National Cancer Center, Koyang, South Korea*
[d]*Department of Radiology, Seoul National University Hospital, 28 Yongun-dong, Chongro-gu, Seoul, 110-744, South Korea*
[e]*Department of Psychology, Kangwon National University, Chuncheon, South Korea*

Received 15 September 2006; revised 8 March 2007; accepted 12 March 2007
Available online 28 March 2007

Parasagittal or off-midsagittal structures of the interhemispheric fiber tracts, i.e., the corpus callosum (CC), have a tendency to form structures which diverge from the midsagittal CC (mCC). This has led to mild inconsistencies in terms of defining parasagittal structures as region of interest for diffusion tensor imaging (DTI) analysis. Moreover, it is a labor-intensive work with potential inconsistencies and inaccuracies to define the parasagittal structure slice by slice using currently available methods. In the present study, to better cope with these problems, a new method was developed to construct the extended parasagittal structure of the CC using diffusion tensor tractography-guided (TGI) parameterization methods based on tract-length-based and parasagittal plane-based extensions. Using extended ROIs, fractional anisotropy (FA) values, as the indicators of fiber integrity in DTI, were compared between normal 14 male (25.7 ± 4.7 years) and 17 female (25.9 ± 4.6 years) groups for investigating the gender difference. Both TGI parameterization methods showed that men have significantly higher regional FA values than women for global CC structure areas in parasagittal and midsagittal space. In contrast, women showed significantly higher FA values in the partial areas of the rostrum, genu and splenium. Our findings based on TGI statistics (TGIS) of fiber integrity could serve as a frame of reference for assessing the group differences of the CCs in finer scale and in more extended space or parasagittal space.

Keywords: Diffusion tensor imaging (DTI); Fractional anisotropy (FA); Corpus callosum (CC); Midsagittal; Parasagittal; Tractography-guided statistics (TGIS); Parameterization

Introduction

In a number of previous studies, the interhemispheric fiber tracts in the corpus callosum (CC) have been selected as a tract of interest because they are the prominent fiber tracts, which interconnect the cerebral hemispheres and play a major role in their integration and are the largest anatomical axonal fiber tract structures (De Lacoste-Utamsing et al., 1985; Witelson, 1989; Witelson and Goldsmith, 1991; Clarke and Zaidel, 1994). There is much evidence to support the notion of considerable gender differences in terms of functional connectivity and anatomical structures. Debates on gender-related dimorphism of the corpus callosum (CC) have centered on findings of a larger splenium in women (De Lacoste-Utamsing and Holloway, 1982) and a larger volume of the CC in the men; however, other reports disagree (Sullivan et al., 2001). In addition, larger volume ratios of CC to forebrain were found in women (Jancke et al., 1997), although this may be explained as an effect of general brain size; men with smaller forebrains have larger volume ratios too. However, a lesser degree of hemispheric lateralization (Cahill et al., 2004) and more bilateral hemispheric activities during cognitive tasks in females than in males (Vikingstad et al., 2000) were reported. In addition, the CC has been addressed in terms of gender differences in its role of interhemispheric integration and specialization (Dorion et al., 2000; Clarke and Zaidel, 1994).

The CC has been subdivided based on geometric considerations in a number of studies (Witelson, 1989; Witelson and Goldsmith, 1991; Jancke et al., 1997; Meisenzahl et al., 1999; Wu et al., 1993) and on shape-based parameterization (Denenberg et al., 1991; Peters et al., 2002). However, most of these studies focused only on the midsagittal CC (mCC) and few regional fiber integrity analysis studies have been performed. Diffusion tensor imaging (DTI) is a new technique for investigating anatomical connectivity

* Corresponding author. Fax: +82 2 3676 2821.
E-mail address: icsong@radcom.snu.ac.kr (I.C. Song).
Available online on ScienceDirect (www.sciencedirect.com).

1053-8119/$ - see front matter © 2007 Elsevier Inc. All rights reserved.
doi:10.1016/j.neuroimage.2007.03.020

and integrity using fractional anisotropy (FA) which is the parameter most frequently investigated in DTI. The FA is generally believed to be representing fiber integrity and can be estimated by DTI. Although there has been a sophisticated imaging technique of magnetization transfer ratio (MTR) imaging for more correctly imaging myelinization, myelinization is not always along with fiber integrity; for example, the FA values of nonmyelinated olfactory nerves were found to be not significantly different from those of other myelinated nerves (Shin et al., 2005). In our previous study, the shape and FA homogeneity-based parcellation of the mCC was conducted using DTI (Oh et al., 2005). In addition, a more recent study on gender difference was conducted by structural MRI and DTI (Shin et al., 2005).

According to Luders et al. (2006), although there are a lot of literatures on significant relationships between the areas of the mCC and the degree of interhemispheric transfer, functional lateralization, and structural brain asymmetries, few studies have examined if callosal asymmetries in parasagittal space (i.e., those close to the brain midline) are related to specific functional consequences. Moreover, the parasagittal structures of the CC have a diverging shape from the mCC; tractographic CC results show that some parts of them go to medial cortices and others to temporal regions (Hofer and Frahm, 2006); this is a common sense rather than a newly found fact. Therefore, there can be mild inconsistency in defining parasagittal CC (pCC) structures as an extended analysis of one on mCC. Moreover, the labor intensiveness and potential inconsistencies/inaccuracies in terms of defining the pCC structures slice by slice hindered the extension of the 2-D mCC study to the 3-D pCC study.

In a previous callosal parcellation study, the differences in callosal connectivity to-and-from cortical/subcortical areas were investigated using brute force tractography (Huang et al., 2005). In contrast, to better describe the intermediate information of calloso-cortical connectivity or pCC structures, a new method for defining extended parasagittal CC structures by tractography-guided manner was developed in the present study. In addition, we developed TGI statistics (TGIS) to better analyze FA gender differences in the pCC and mCC.

Although there is a recent study on tract-based spatial statistics (TBSS), it is focused on using the skeletal shape of mean FA maps to represent mean fiber tracts (Smith et al., 2006). Another representative tract parameterization study utilized a scale-invariant parameterization by DT tractography of the cingulum bundle based on anterior commissure (AC) and posterior commissure (PC) points and angular divisions (Gong et al., 2005). However, this method involves the geometry-based parameterization of fiber tracts which are already reconstructed from the non-parameterized 2-D seed regions. To the best of our knowledge, the present study is the first to use an initial ROI parameterization and a TGI parameterization for spatial statistics in specific fibers of interest. These two parameterization methods have important meanings for quantitative and consistent studies on the mCC and pCC.

Materials and methods

Participants

To avoid potential handedness- or age-related dimorphism of the CC, age matched right handed young healthy volunteers were recruited: 14 males (25.7±4.7 years) and 17 females (25.9±4.6 years).

Data acquisition

All data were obtained using a double spin echo planar imaging sequence on a GE 3.0 T imaging system; diffusion weighted images with 25 noncollinear diffusion gradients and without diffusion gradient were acquired. For convenience, images without a diffusion gradient are referred to as B_0 images. The scan parameters used were TR/TE= 10,000/90 ms, b=1000 s/mm^2, matrix=256×256, FOV=240 mm, axial slice thickness=4 mm (with no gap), 1 NEX. To better compensate for the poor interslice resolution, the authors interpolated the image volume along with slice direction to be spatially isotropic.

Image processing

As summarized in Fig. 1, image volumes were processed using a number of manual and automated image processing procedures including: (1) spatial normalization of DTIs for midsagittal slice selection; (2) defining mCCs in normalized FA maps; (3) parameterization of the mCC, i.e., constructing a parametric mesh of the mCC using a boundary model-based shape description (Denenberg et al., 1991; Peters et al., 2002; Oh et al., 2005); (4) constructing a template parametric mesh of the mCC followed by the spatial normalization of an individual parametric mesh onto this template mesh; (5) inverse deformation of seed points from template mCC space to individual mCC space; (6) tractography with fiber assignment by the continuous tracking (FACT) algorithm (Mori et al., 1999); (7) parameterization of the resulting fiber tracts using tract-length-based (7-a) and parasagittal plane-based (7-b) extensions; (8) obtaining FA values on parametric mesh of the pCC as well as that of the mCC; and (9) statistical analysis using a two-sample t-test on FA values of all nodes in parametric meshes.

Spatial normalization for midsagittal slice selection and mCC extraction

In previous studies, in an effort to better cope with the mCC selection, several methods including MRI acquisition along AC–PC line and manual or automatic refinements after visual inspection (Huang et al., 2005) have been utilized. To more objectively and consistently select midsagittal slices to define an mCC object without these additional efforts, spatial normalization was conducted as described by Peters et al. (2002). For more accurate spatial normalization with reducing spatial mismatch due to ethnic brain dimorphism, the specific B_0 (SSB_0) template image was used as emphasized in a recent optimized voxel-based morphometry (OVBM) study (Good et al., 2001). A midsagittal slice was selected in normalized DTI space, i.e., template image space. Since DTIs are already spatially normalized, iterative refinement of AC–PC alignment (Huang et al., 2005) is unnecessary for delineating the mCC. The degree of freedom (DOF) of the spatial normalization was 12 parameters, i.e., affine transform only. As a *post hoc* spatial normalization of a CC object rather than its image will be conducted on this mildly spatial normalized DTI in the Estimation of deformation field between template and individual parametric meshes section, a low DOF does not matter. All mCCs were manually defined on an FA weighted color-coded map on midsagittal slices.

Parameterization of the mCC

From the extracted mCC, its parametric mesh was constructed using a boundary model-based shape description (Denenberg et al.,

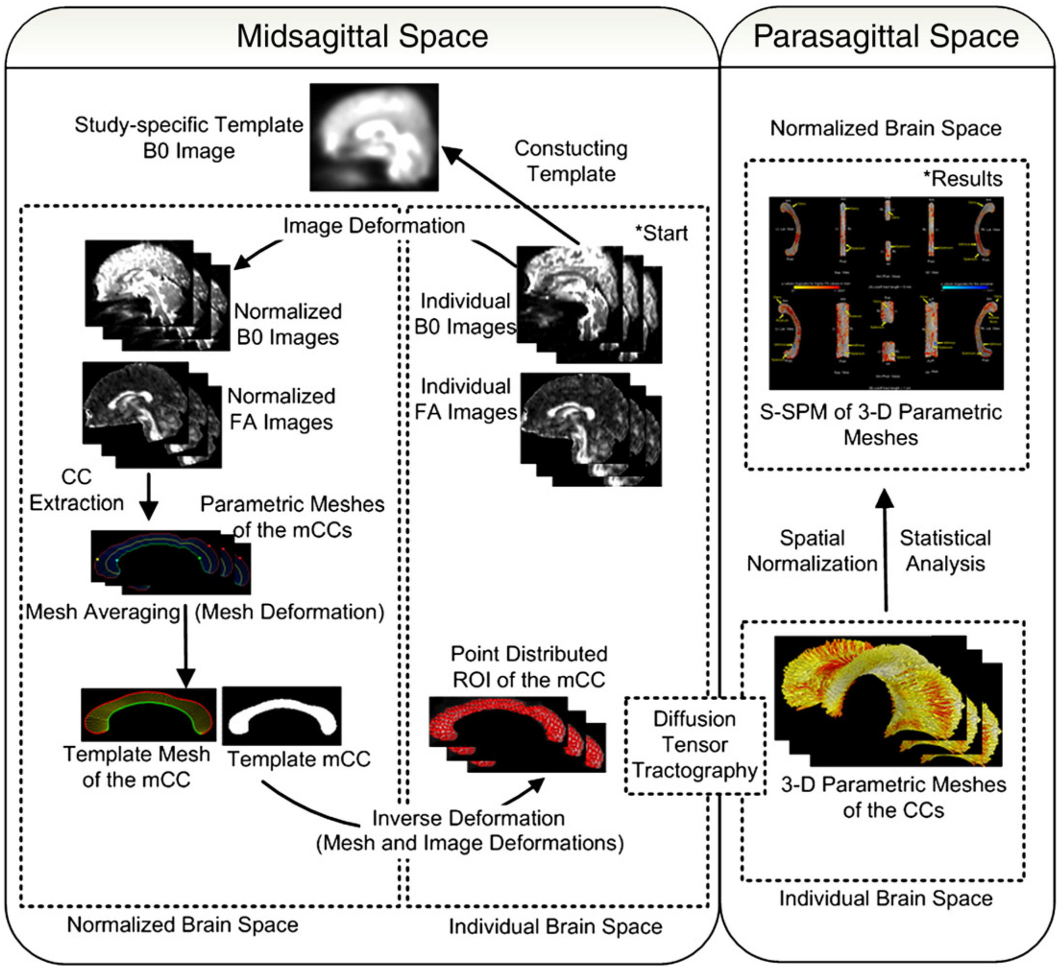

Fig. 1. Block diagram for image processing and statistical analysis. Footnote: point-distributed ROIs, i.e., parametric seed points in the mCC were extracted using two step inverse deformation, i.e., mesh inverse deformation and image inverse deformation. Each step of block diagram contains an example of original data. Using tractography, data in midsagittal space can be extended into parasagittal space. Abbreviation: mCC: midsagittal corpus callosum; pCC: parasagittal corpus callosum.

1991; Peters et al., 2002; Oh et al., 2005). As suggested by Peters et al. (2002) and as adopted in our pervious study (Oh et al., 2005), the high curvature regions of genu and splenium were treated separately. In these studies, four control points were commonly used such that the sum of percentile widths is minimized; as a result, global shape with high curvature in genu and splenium was well represented, and corresponding points on the upper and lower contours were approximately perpendicular to the medial axis in the global aspect.

Construction of the mCC template

From the constructed parametric meshes of individual CCs, their template was constructed. Spatial transform with four parameters, i.e., 2-D rigid body transform, was applied to individual parametric meshes such that the line that connects anterior and posterior tips of the CC was aligned to horizontal line and that the sizes of the CC became their mean value.

Estimation of deformation field between template and individual parametric meshes

Although deformation fields between template and individual parametric meshes can be estimated by using the coordinates of all nodes in parametric meshes, a method for estimating deformation fields is needed in equivocal voxels, which are not on the nodes of parametric mesh. As one can estimate deformation fields between individual and template CCs by spatial normalization or warping, the current procedure is equivalent to conducting the warping of an individual CC object onto a template CC object. Unlike a sophisticated and rigorous method (Huang et al., 2005) for warping individual CCs onto template or representative CCs using *Large Deformation Diffeomorphic Metric Mapping* (LDDMM), focusing on TGI parameterization of the pCC, we used thin-plate spline (TPS) interpolation (Bookstein, 1989). TPS interpolates a set of irregularly sampled data value over a regular two-dimensional grid to resolve the current warping problem. In addition, it is an ideal method for modeling complex local deformation fields, which are too complex to be represented by polynomials. A similar method of cubic spline interpolation was briefly addressed in our previous DTI study on the subdivision of the mCC (Oh et al., 2005).

Voxelwise ROI on the mCC template and corresponding point-distributed ROIs on individual mCCs

Parametric mesh-based seed point selection provides the same number of seed points for all subjects. However, this mesh does not have an isotropic grid even in template CC space. To produce a more familiar data format for neuroimaging scientists, voxelwise seed points in template CC space were extracted. The finer parametric mesh gets the closer to or equal to a voxel one can sample a node of mesh. Using this method, seed points became voxelwise data at least in the template space. Using an inverse transform of CC object-based spatial normalization, seed points in template space can be transformed into individual space in order to be used as seed points of the mCC for tractography.

Parameterization of the pCC using tractographic extension methods

As mentioned above, the mCC object and its parametric mesh can be easily extracted using the parameterization techniques mentioned above. The constructed parametric mesh of an mCC can be directly extended to parasagittal space as guided by diffusion tensor tractography. Consequently, the TGI parameterization of mCC and pCC could be completed (Fig. 2).

Tractographic extension was performed using two sampling techniques: (1) parasagittal parallel plane-based sampling with a step size of 1 mm, which mimics previous pCC shape analyses (Narr et al., 2000; Luders et al., 2006), and (2) tract-length-based sampling with unit length of 1 mm which is performed by resampling tractograms. The step size and the unit length of 1 mm were equal to the voxel size of normalized DTI space, i.e., SSB_0 space.

Surface-based statistical parametric mapping (S-SPM)

As our devised method uses CC objects only, i.e., masked images of the CC or a parametric mesh with a zero-valued background, volumetric smoothing would cause an erroneous result. Even after considering backgrounds as non-zero valued images, the CC is surrounded by gray matter (GM), corticospinal fluid (CSF), and other fiber tracts, such as the fornix and cingulum tracts. Therefore, the CC can be potentially contaminated by the partial volume effect (PVE) by other structures when voxel-based smoothing is applied to it. To avoid this unwanted effect, surface-based smoothing was employed as preprocessing for surface-based SPM. In the present study, diffusion smoothing (Chung et al., 2001; 2003), which is an extended form of Gaussian smoothing for surface manifolds, was used (FWHM = 5 mm). Subsequently, the two-sample *t*-test was conducted to statistically compare FA values in corresponding nodes on the 3-D parametric tractography meshes.

Results and discussion

A new TGI parametric mesh in 3-D

Although there was a previous study which used above-mentioned TBSS, it was based on medial model-based description, i.e., the skeletal shape of mean FA map with the indirect information of fiber tracts, i.e., mean FA map to represent mean fiber tracts (Smith et al., 2006). Generally, the medial model-based shape description has strength in describing global shape of object but weakness in describing local details. In contrast, our method is based on a more balanced boundary model-based shape description which adopted the merit of skeletal shape-based method in the sense that it used four control points to better describe global shape as compared to the boundary model-based shape description only. The strength of the balanced boundary model-based shape description in the CC study has been validated in a number of studies (Denenberg et al., 1991; Peters et al., 2002; Oh et al., 2005). In addition, our method is directly based on the fiber tracts, i.e., tractographic extension.

In the previous approach of Gong et al. (2005), the tractography was used for reconstructing fiber tracts of cingulum bundle, and

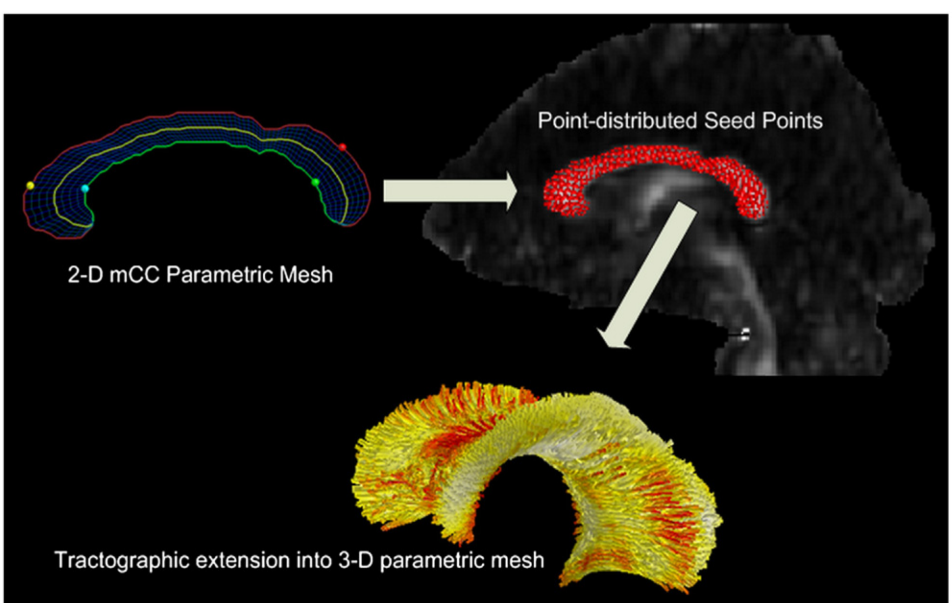

Fig. 2. Enlarged view of parametric mesh of the mCC, point-distributed ROI, and its tractography-guided extension to the pCC. Footnote: a representative example for tractography-guided extension from 2-D parametric mesh and seed points into 3-D parametric mesh is depicted. Four spheres represent the control points. Abbreviation: mCC: midsagittal corpus callosum; pCC: parasagittal corpus callosum.

within-tract positions were used for parameterizing the FA values on the tract. In contrast, our devised method is based on two kinds of parameterization; first, the parameterization of initial seed points, i.e., starting points of tractography at the mCC which is determined by both CC shape specific description and the deformation field as described in sections from Parameterization of the mCC to Estimation of deformation field between template and individual parametric meshes; second, the parameterization of the pCC using tract-length-based extension which is corresponding to the within-tract position-based parameterization of Gong's approach. Regarding the detail of differences between the previous methods and ours, although both Gong's method and ours employed the hand-drawn ROI, our method parameterized not only the reconstructed fiber tracts but also the initial ROI. Unlike Gong's approach, our spatial statistics was implemented by parameterizing them not one-dimensionally but three-dimensionally; (1) Gong's one-dimensional parameterization of FA values is an arc angle-based method for one fiber bundle rather than one tractographic line; this can be re-entitled 'tractographic extension of *lumped* cross-sectional ROI analysis'; (2) Our three-dimensional parameterization of FA values in midsagittal seed points and their tractographic extension to the parasagittal space can be re-entitled 'tractographic extension of *parameterized* cross-sectional ROI analysis'.

In our previous study (Oh et al., 2005), we mentioned the need to extend the ROI of the mCC into the pCC and for tractography-based mapping between the mCC and the cortex. In the present study, in order to analyze fiber integrity in the pCC, a new tractography-guided extension of a 2-D parametric mesh of the mCC into a 3-D mesh was performed. In addition, fiber integrity levels, i.e., the FA values of mCC and pCC, which cannot be investigated in structural MR images, such as 3-D spoiled gradient echo (SPGR) or magnetization prepared rapid gradient echo (MPRAGE) images, were investigated in across-group comparisons using DTI. In addition, the devised method can be easily accommodated to provide a rigorous shape analysis technique on fiber tracts with curvature, torsion and Fourier descriptions (Batchelor et al., 2006) because we have already parameterized the 3-D structures of the mCC and pCC. As mentioned above, a previous study by Huang et al. (2005) was focused on terminal-to-terminal information, i.e., mCC and the cortical surface. Therefore, it has strength in functionally homogeneous region-based CC parcellation. However, the parcellated results have very high interindividual variability; it is not easy to adopt Huang's method for investigating the intermediate CC structure with one-to-one mapping. In contrast, the present study uses intermediate information only. However, the current method has strength in intersubject mapping of corresponding fiber tracts using CC shape-specific parameterization. In addition, the previous study on the cortical parcellation-based CC parcellation has substantially less robustness in terms of tracking gray matter regions or diverging fiber tracts in the CC because it used maximum likelihood orientation-based deterministic tracking.

In future studies, to overcome the abovementioned limitations and to perform more accurate mapping between the CC and gray matter areas, including cortical and subcortical areas, probabilistic tractography such as the one performed by Behrens et al. (2003) should be used for more robust tracking given the uncertainty of fiber orientation in cortical/subcortical regions and diverging CC regions.

Parasagittal CC has only been so far reported on by Luders et al. (2006). These workers employed surface-based thickness measurements for assessing hemispheric asymmetry in finer scale. Although they adopted an anatomical surface-based mesh modeling method to model pCC, this method cannot be satisfactorily used for regions distanced from mCC. In their study, parasagittal slices were used for analysis on callosal asymmetry, which were 6 mm away from the mCC. In addition, as callosal extension is conducted by using finer slices, for example using parasagittal slices with a thickness of 1 mm, it would be tremendously labor intensive to define CC objects in each slice. The current method provides a substantially new TGI parameterization-based way to better cope with these works in an automated manner.

Why parameterization?

Whereas the majority of shape parameterization techniques focused on surface shape analysis in the cortical surface or basal ganglia (Fischl et al., 1999; Hwang et al., 2006), a number of studies have been performed on parameterization of the 2-D mCC (Witelson, 1989; Witelson and Goldsmith, 1991; Denenberg et al., 1991; Wu et al., 1993; Jancke et al., 1997; Meisenzahl et al., 1999; Narr et al., 2000; Peters et al., 2002; Oh et al., 2005). In addition, at least two studies have been conducted on the parameterization (Gong et al., 2005) and shape analysis (Batchelor et al., 2006) of fiber tracts. Since there are many intersubject differences in terms of the size and shape of the CC, it is unfair to use a whole CC mask as seed points for tractography in all subjects. Although Huang used *post hoc* spatial normalization of the dominance map (Huang et al., 2005), it was based on a warping of the tractographic result from the individual brain space into template brain space; as a result, the tractograms of individual subject will have a different numbers of seed points. In contrast, our parameterization method is based on the one-to-one mapping of seed points in both individual and normalized brain spaces. Consequently, *corresponding points* on the 3-D parametric mesh of all subjects were ready for statistical analysis. In addition, our parameterization in the ROI allowed us to analyze the CC with very fine scale as a number of voxel-based studies such as voxel-based (VBM) and deformation-based morphometries (DBM). Although traditional DBM studies may seem to be similar to the present method, they are generally based on the image intensity of the whole brain rather than the exact matching of the CC object. In contrast, our method is based on CC shape-specific description and it seems to be an anatomically more salient method than the intensity-based one. In addition, our study is DTI tractography-based three-dimensional extension rather than voxel-based three-dimensional extension. In these senses, the authors think that current method is anatomically salient than conventional methods. As mentioned above, although the previous study of Gong et al. (2005) used a tractographic parameterization of fiber tracts, within-ROI information was a one lumped such as mean and standard deviation (SD) of FA values. In contrast, our method can be used for investigating the CC in a voxel-scale as in the voxel-based analysis because the seed points on the template CC space were sampled voxel by voxel. Moreover, as cingulum bundles are dispersed widely in the most anterior and posterior portions, Gong's approach was only applicable to the part of the tract dorsal to the CC (Gong et al., 2005). With using within-ROI parameterization, this limitation on ROI of reconstructed fiber tracts can be resolved because of one-to-one mapping, i.e., correspondence between initial seed points and fiber tracts.

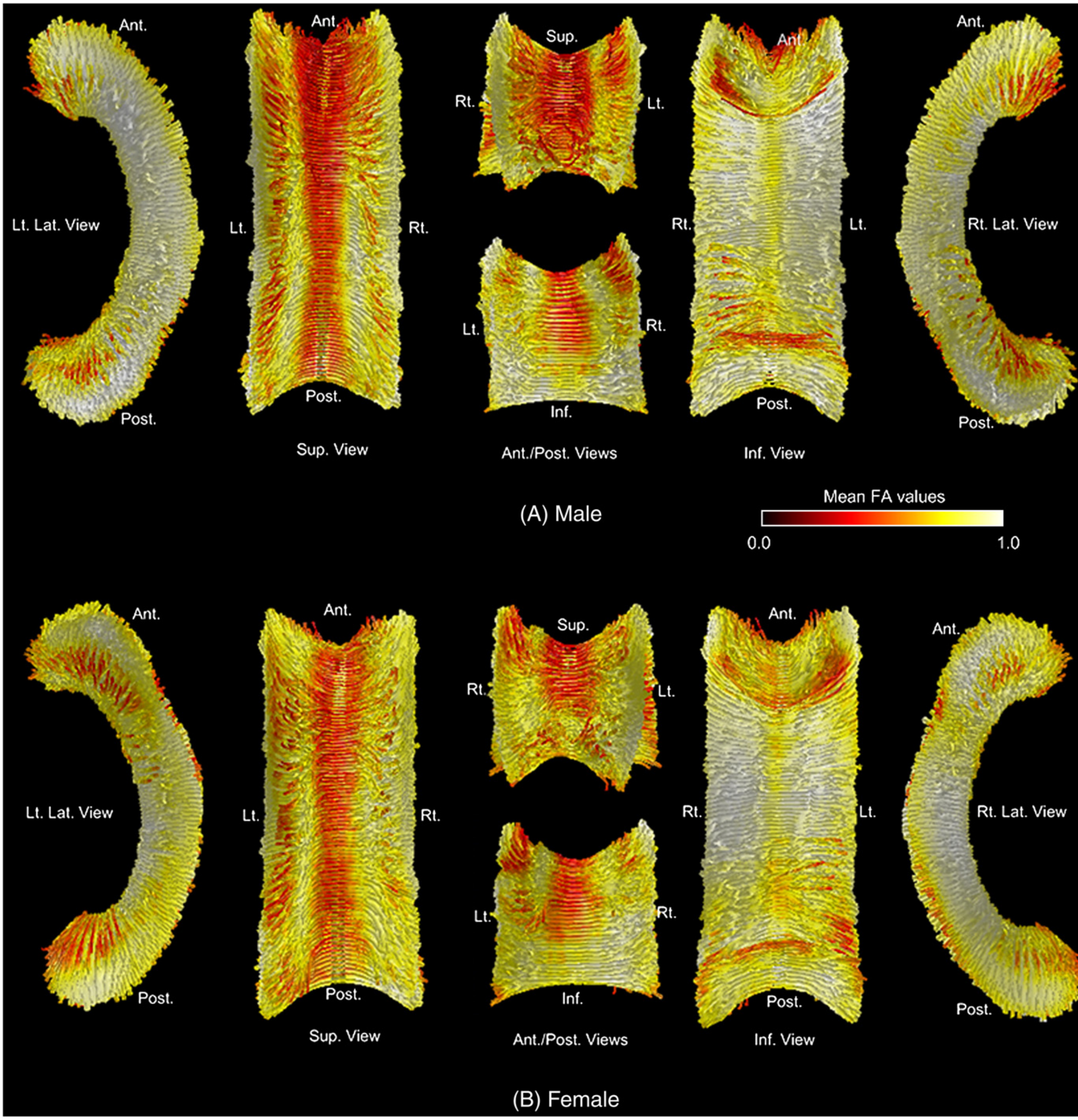

Fig. 3. Gender difference of regional mean fractional anisotropy (FA) values represented in a color-coded fashion and hypertensor visualization using streamtube. Footnote: the thickness of streamtube was modulated using FA values of its composing points, such that points with lower FA values are represented as thinner tubes. The mean parametric meshes of male (A) and female (B) groups are depicted. Abbreviation: Sup.: superior; Inf.: inferior; Ant.: anterior; Post.: posterior; Lat.: lateral, Lt.: left, Rt.: right.

Modes of failure and success of tractographic extension

Regarding the failure mode of tractographic extension, the current subjects have not shown any failure mode of tracing adjacent fiber tracts such as cingulum bundle or fornix. In our application studies in other pathological and pediatric groups showed some erroneous results of this kind in the midbody of the CC. However, a rule-based solution for this failure mode to separately process the midbody parts of the CC in erroneous case is already equipped and it may be out of the scope of the current study and will be conducted as further study. Since other prior stages of tractographic extension were already validated in the previous studies of Denenberg et al. (1991), Peters et al. (2002) and ours (Oh et al., 2005), they were omitted. For the similar reasons, the validations for surface-based smoothing and S-SPM were also omitted.

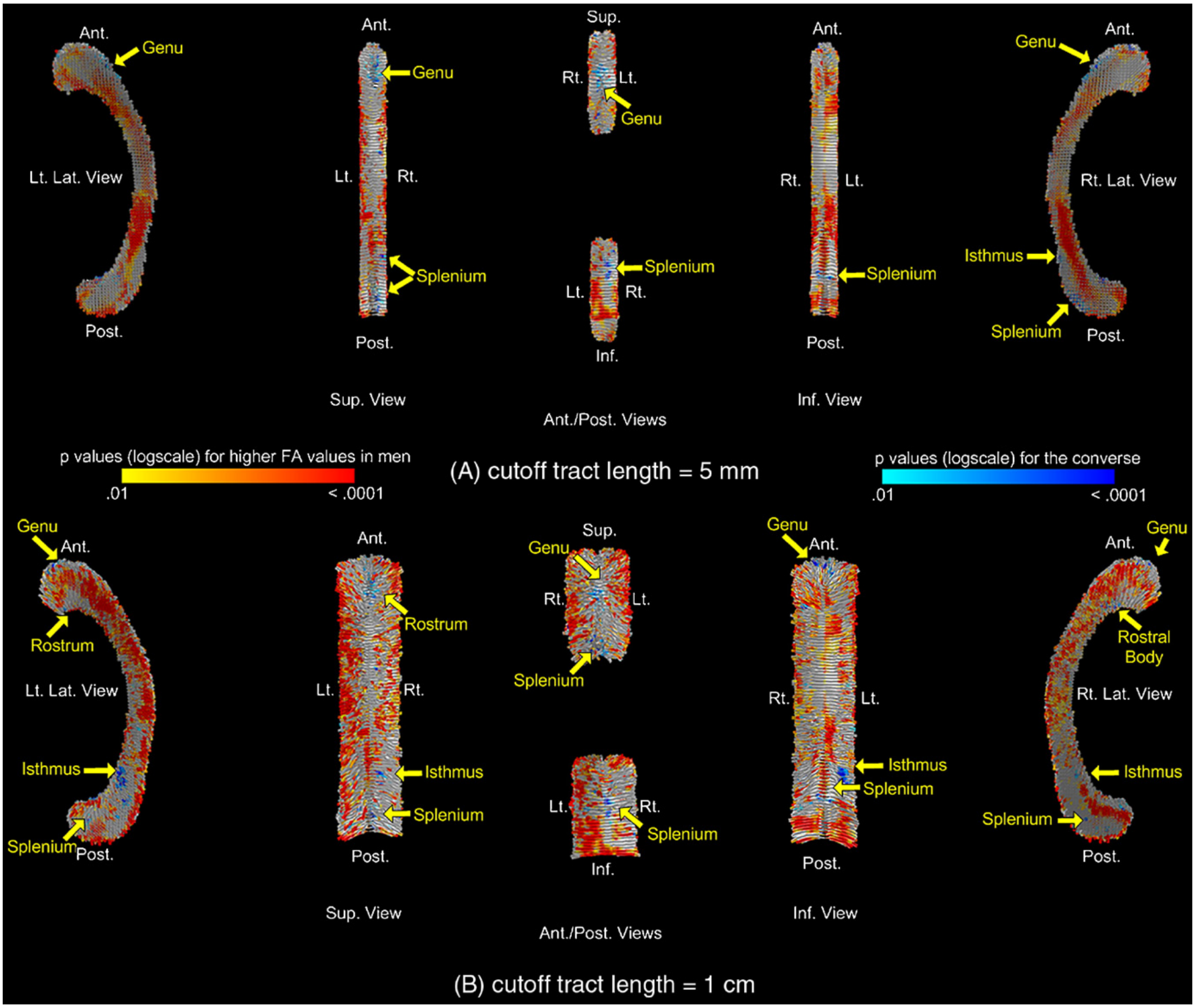

Fig. 4. Illustration of the results of regional fractional anisotropy (FA) gender difference: tract-length-based cutting at 5 mm (A) and 1 cm (B) from seed points. Footnote: for better visual inspection, various aspects of the reconstructed fiber tracts were depicted. Yellow to red areas represent regions where the FA level of men was found to be significantly higher than that of women; the converse is shown as cyan to blue (see color bars). Abbreviation: Sup.: superior; Inf.: inferior; Ant.: anterior; Post.: posterior; Lat.: lateral, Lt.: left, Rt.: right.

Mean parametric mesh for visualizing the average shape and average FA values

In order to average fiber tracts into one tract with a mean shape, the averaged coordinates of corresponding points in tractographic space were used; the mean coordinates of each node in parametric CC meshes were obtained from male and female groups to construct the group mean for parametric CC meshes.

In a previous study which employed averaged tractography in volumetric space (Park et al., 2003), mean fiber tracts were constructed from spatially normalized DTIs. As they emphasized the important fact that DTI consists of multiple-channel information such as orientation and anisotropy, DTI provides a number of images with vector quantities. Therefore, naive spatial transforms cannot maintain the original anatomical correspondence and a rigorous tensor reorientation procedure is required for appropriate spatial transformation of DT images (Park et al., 2003; Xu et al., 2003). In addition, some literatures including the recent one by Park et al. (2003) showed that iterative spatial transform and tensor reorientation to minimize registration errors may require much computational time.

To better cope with resampling tractography in normalized brain space after affine transformation, 10 times supersampling of tractograms was conducted and followed by the affine transform. Affine transform (as conducted for midsagittal slice selection) was applied to tractography in individual brain spaces to remove the global interindividual misalignments of individual DTI's. The presence of residual spatial mismatch, which is generally removed by nonlinear warping in the previous studies, can reduce the accuracy of mean tractogram construction in tractographic space. However, this is a minor concern because the constructed mean tractogram is not used for analyzing the shape of tractogram but only for visualizing statistical results.

As depicted in Figs. 3–5, mean FA values are globally high in males according to the report of Shin et al. (2005). However, those

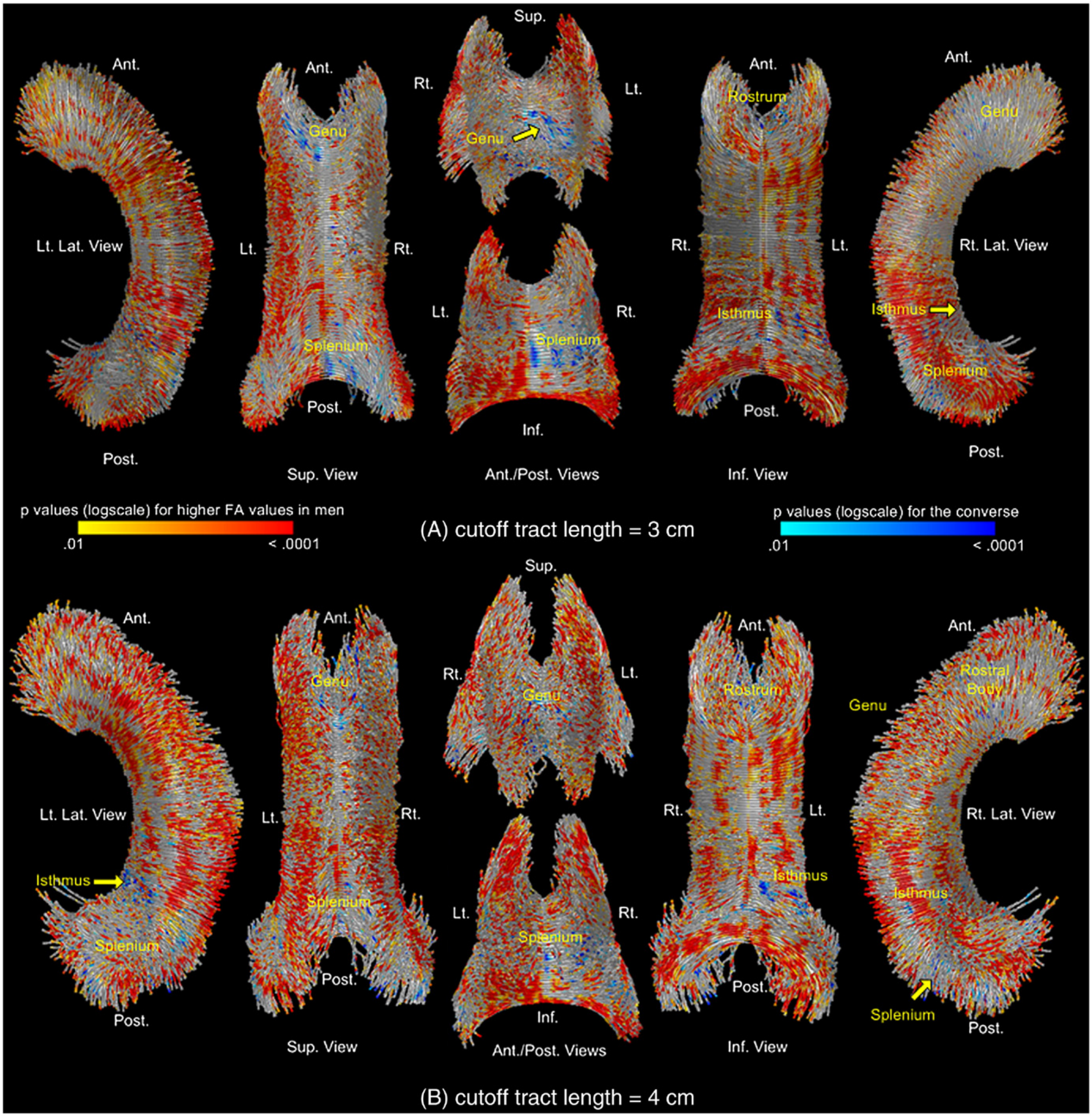

Fig. 5. Gender effect by regional fractional anisotropy (FA) values: tract-length-based cutting at 3 (A) and 4 cm (B) from seed points. Footnote: all visualization parameters are as for Fig. 4. Abbreviation: Sup.: superior; Inf.: inferior; Ant.: anterior; Post.: posterior; Lat.: lateral, Lt.: left, Rt.: right.

in small regions of the anterior and posterior CC, i.e., some parts of genu, rostrum, isthmus and splenium (arrowed regions in Figs. 4 and 5) which were not detected in the previous study of Shin et al. (2005), were low. In addition, women had relatively more regions with higher FA values than men in the upper parts of CCs, although men had higher FA values than women in more regions even in the upper parts of CCs. The results illustrated in Figs. 4 and 5 show that our method is powerful at virtually dissecting, i.e., an interactive cutting of the CC in any directions with respect to tract lengths from the seed points or distances from mCC. If we had used the conventional methods only, it would have taken several hours to define all mCC and pCC objects slice by slice and potential inconsistencies and inaccuracies accompanying it would be more serious problems.

Whereas Shin et al. (2005) reported the effect of gender on fiber integrity based on the classical and conservative Witelson's method (Witelson, 1989; Witelson and Goldsmith, 1991) for the geometric subdivision of the CC using vertical lines, our finer parametric mesh-based parcellation using FA homogeneity as suggested in our previous study (Oh et al., 2005) produced mildly different patterns from those of Witelson's method. Moreover, our devised method represents an extension of our previous method in midsagittal space. Therefore the current method is more sensitive to FA value regional differences than Witelson's method. Consequently, it will better facilitate DTI studies of intergroup differences.

S-SPM

Spatial smoothing is generally used to increase signal to noise ratio (SNR) and the Gaussianities of image intensities and for accommodating potential spatial mismatch induced by incorrect image coregistration (Park et al., 2006). Recently, surface-based statistical probabilistic mapping (S-SPM) has been widely applied in the neuroimaging field because of its efficacy at representing features in the cortical surface manifold (Chung et al., 2001, 2003; Park et al., 2006). Moreover, Park et al. (2006) applied this method to partial volume correction and statistical analysis for metabolic activation using ^{18}F-FDG positron emission tomography (PET) images. These methods have particularly advantages for structures with a high curvature like the cortical surface. Although the surface generated by TGI parameterization is relatively smooth with little curvature, there can be also PVE, as mentioned above, when volumetric smoothing is applied. Therefore, the S-SPM was utilized in the present study.

Statistical results of S-SPM

To investigate the statistical significance of mean FA levels by their visual inspection, the color-coded significance of S-SPM is depicted in Figs. 4 and 5. Shin et al. (2005) reported that the subregional FA values were globally higher in males and significantly higher in genu ($p<0.01$) and posterior body ($p<0.05$). In the present study, approximately 42% of the regions in which the statistical analysis was conducted were found to show a significant ($p<0.01$) gender difference with respect to fiber integrity; globally higher FA values in males as compared to females have been detected in voxels with significance of $p<0.01$ and some voxels were even significance of $p<0.0001$ (red colored regions in Figs. 4 and 5). Regions with a significant gender difference were represented as color-coded in Figs. 4 and 5 and higher FA values in female group were represented as yellow words and arrows. The authors found that gender differences as determined by mean FA levels in the previous section Mean parametric mesh for visualizing the average shape and average FA values concurred gender differences by significance mapping. As discussed by Aboitiz et al. (1992) and Shin et al. (2005), the isthmus is known to exhibit a higher proportion of large fiber and to have lower FA values and genu/splenium possesses the densest thin fibers and higher FA values. In an analogy to this fact, there is a possibility that males have a higher proportion of more densely packed thin fibers across the global CC than females (Shin et al., 2005). In addition, higher amounts of interconnecting fiber tracts between functionally different areas (Shin et al., 2005) in females as compared to males, which is relevant to a lesser degree of hemispheric lateralization (Cahill et al., 2004) and more bilateral hemispheric activities during cognitive tasks (Vikingstad et al., 2000) in females, can be thought as another factor of the gender difference of FA values. The reverse results of higher FA values in females than in males for some regions may suggest that these factors can be regionally reversed in both groups.

Limitations and further studies

In the present study, a maximum likelihood orientation-based tracking algorithm (FACT; Mori et al., 1999) was used for one-to-one mapping between mCCs and pCCs. Therefore, brute force tractography (Huang et al., 2004), which allows mapping multiple fiber tracts onto one seed point, was not used, although it is more robust for tracking crossing fiber tracts than FACT. However, this assumption can not be guaranteed for the whole CC, which is even connected to the cortical surface and subcortical areas (Huang et al., 2005). Furthermore, a rigorous validation of one-to-one mapping in near-midsagittal and far-midsagittal spaces should be conducted. As discussed by Smith et al. (2006), the current method also has the same limitation of previous tractographic parameterization-based methods; these methods can be used in investigating only those tracts that can be reliably traced and be separated from other tracts. Since the present method is based on the one-to-one mapping of corresponding points, i.e., midsagittal starting points and parasagittal intermediate points, it is inappropriate to apply this method to fiber tracts with more complicated structures, such as crossing fibers (e.g., U-shaped fibers). To resolve this problem, the technique of the high angular diffusion (HARD) imaging including q-ball imaging (Tuch, 2004), which is better equipped to deal with multiple fiber tracts population in a single voxel, can be used. Additional candidates for solving the diverging tract problem are brute force tractography (Huang et al., 2004) and probabilistic tractography (Behrens et al., 2003), which are both capable of mapping multiple fiber tracts on a single voxel.

More importantly, the current method has limitation of not using functional homogeneity-based parcellation such as a cortical parcellation-based CC parcellation study conducted by Huang et al. (2005). As mentioned above, the results of functional homogeneity-based parcellation have high interindividual variability in 2-D mCC space. Therefore, a new compromising method which can keep functional homogeneity information and conduct effective parameterization should be developed in the near future.

Given the assumption that one-to-one mapping is well defined, generalization to other fiber tracts can be easily conducted. In addition, using template-based automatic ROI selection for tractography, as conducted by Thottakara et al. (2006), diverging fibers from converged ROIs can be well parameterized using our devised TGI method.

Although rigorous correction for multiple comparisons, such as Gaussian random field or false discovery rate (FDR) modalities, were not applied during the present study, we believe that the present results are of value in a sense that the present study is on methodology rather than clinical application and the threshold for significance ($p<0.01$) and the number of participants are reasonable. In addition, although there are controversies on the normality, i.e., Gaussianity of FA values as (1) the number of subjects is relatively large (14 males and 17 females); (2) appropriate Gaussian smoothing (FWHM = 5 mm) was applied; and (3) a number of previous studies assumed the Gaussianity of FA values for these reasons, we conducted spatial statistics based on normality.

Conclusion

The present article represents the first DTI study in the CC using TGI parameterization. In the present study, the authors propose a new method for analyzing the pCC and the mCC by TGI parameterization and its surface-based SPM. Our TGI parameterization which used parasagittal plane-based and tract-length-based extensions revealed that men were found to have significantly higher regional CC FA values than women, i.e., in the pCC and mCC spaces. In contrast, women showed significantly higher FA values in small parts of anterior and posterior regions, i.e., some parts of genu, rostrum, isthmus and splenium than men. The present study is the first to extend conventional 2-D mCC-based analysis to 3-D parametric mesh of mCC and pCC in a tractography-based quantitative manner. Given the potential of our devised technique as a frame of reference, the authors suggest that it will find a number of pathology-related applications. Moreover, tract-length-based parameterization of the pCC can at present be performed using only our method, and the substantial physical meaning of anatomical correspondences (Park et al., 2003) is likely to be much greater in our method than in the previous geometric division, i.e., parasagittal the plane-based method. In addition, *virtual dissection* of reconstructed parametric tractogram can be conducted in any wanted directions. Our method is more anatomically salient than currently available other methods, and therefore potentially more representative in physical terms with respect to anatomical correspondences. Moreover, the current method will be more useful when the parasagittal extension is conducted toward further lateral direction.

Acknowledgments

The current research was supported in finance partially by the Brain Research Center of the 21st Century Frontier R&D Program (M103KV010016-06K2201-01610) and by the Korea Research Foundation Grant funded by the Korean Government (MOEHRD) (KRF-2006-352-D00220).

Appendix A. Supplementary data

Supplementary data associated with this article can be found, in the online version, at doi:10.1016/j.neuroimage.2007.03.020.

References

Aboitiz, F., Scheibel, A.B., Fisher, R.S., Zaidel, E., 1992. Fiber composition of the human corpus callosum. Brain Res. 598, 143–153.

Batchelor, P.G., Calamante, F., Tournier, J.-D., Atkinson, D., Hill, D.L., Connelly, A., 2006. Quantification of the shape of fiber tracts. Magn. Reson. Med. 55, 894–903.

Behrens, T.E., Johansen-Berg, H., Woolrich, M.W., Smith, S.M., Wheeler-Kingshott, C.A., Boulby, P.A., Barker, G.J., Sillery, E.L., Sheehan, K., Ciccarelli, O., Thompson, A.J., Brady, J.M., Matthews, P.M., 2003. Non-invasive mapping of connections between human thalamus and cortex using diffusion imaging. Nat. Neurosci. 6, 750–757.

Bookstein, F.L., 1989. Principal Warps: thin-plate splines and the decomposition of deformations. IEEE Trans. Pattern Anal. Mach. Intell. 11, 567–585.

Cahill, L., Uncapher, M., Kilpatrick, L., Alkire, M.T., Turner, J., 2004. Sex-related hemispheric lateralization of amygdala function in emotionally influenced by memory: an FMRI investigation. Learn. Mem. 11, 261–266.

Chung, M.K., Worsley, K.J., Paus, T., Cherif, C., Collins, D.L., Giedd, J.N., Rappoport, J.L., Evans, A.C., 2001. A unified statistical approach to deformation-based morphometry. NeuroImage 14, 595–606.

Chung, M.K., Worsley, K.J., Robbins, S., Paus, T., Taylor, J., Giedd, J.N., Rappoport, J.L., Evans, A.C., 2003. Deformation-based surface morphometry applied to gray matter deformation. NeuroImage 18, 198–213.

Clarke, J.M., Zaidel, E., 1994. Anatomical–behavioral relationships: corpus callosum morphometry and hemispheric specialization. Behav. Brain Res. 64, 185–202.

De Lacoste-Utamsing, C., Holloway, R.L., 1982. Sexual dimorphism in the human corpus callosum. Science 216, 1431–1432.

De Lacoste-Utamsing, M.C., Kirpatrick, J.B., Ross, E.D., 1985. Topography of the human corpus callosum. J. Neuropathol. Exp. Neurol. 44, 578–591.

Denenberg, V.H., Kertesz, A., Cowell, P.E., 1991. A factor analysis of the human brain's corpus callosum. Brain Res. 548, 126–132.

Dorion, A.A., Chantone, M., Hasboun, D., Zouaoui, A., Marsault, C., Capron, C., Duyme, M., 2000. Hemispheric asymmetry and corpus callosum morphometry: a magnetic resonance imaging. Neurosci. Res. 36, 9–13.

Fischl, B., Sereno, M.I., Tootell, R.B., Dale, A.M., 1999. High-resolution inter-subject averaging and a coordinate system for the cortical surface. Hum. Brain Mapp. 8, 272–284.

Gong, G., Jiang, T., Zhu, C., Zang, Y., Wang, E., Xie, S., Xiao, J., Guo, X., 2005. Asymmetry analysis of cingulum based on scale-invariant parameterization by diffusion tensor imaging. Hum. Brain Mapp. 24, 92–98.

Good, C.D., Johnsrude, I.S., Ashburner, J., Henson, R.N., Friston, K.J., Frackowiak, R.S.J., 2001. A voxel-based morphometric study of ageing in 465 normal adult human brains. NeuroImage 14, 21–36.

Hofer, S., Frahm, J., 2006. Topography of the human corpus callosum revisited—comprehensive fiber tractography using diffusion tensor magnetic resonance imaging. NeuroImage 32, 989–994.

Huang, H., Zhang, J., van Zijl, P.C., Mori, S., 2004. Analysis of noise effects on DTI-based tractography using the brute-force and multi-ROI approach. Magn. Reson. Med. 52, 559–565.

Huang, H., Zhang, J., Jiang, H., Wakana, S., Poetscher, L., Miller, M.I., van Zijl, P.C., Hillis, A.E., Wytik, R., Mori, S., 2005. DTI tractography based parcellation of white matter: application to the mid-sagittal morphology of corpus callosum. NeuroImage 26, 195–205.

Hwang, J., Lyoo, I.K., Dager, S.R., Friedman, S.D., Oh, J.S., Lee, J.Y., Kim, S.J., Dunner, D.L., Renshaw, P.F., 2006. Basal ganglia shape alterations in bipolar disorder. Am. J. Psychiatry 163, 276–285.

Jancke, L., Staiger, J.F., Schlaug, G., Huang, Y., Steinmetz, H., 1997. The relationship between corpus callosum size and forebrain volume. Cereb. Cortex 7, 48–56.

Luders, E., Narr, K.L., Zaidel, E., Thompson, P.M., Jancke, L., Toga, A.W., 2006. Parasagittal asymmetries of the corpus callosum. Cereb. Cortex 16, 346–354.

Meisenzahl, E.M., Frodl, T., Greiner, J., Leinsinger, G., Maag, K.P., Heiss, D., Hahn, K., Hegerl, U., Moller, H.J., 1999. Corpus callosum size in schizophrenia—a magnetic resonance imaging analysis. Eur. Arch. Psychiatry Clin. Neurosci. 249, 305–312.

Mori, S., Crain, B.J., Chacko, V.P., van Zijl, P.C., 1999. Three-dimensional tracking of axonal projections in the brain by magnetic resonance imaging. Ann. Neurol. 45, 265–269.

Narr, K.L., Thompson, P.M., Sharma, T., Moussai, J., Cannestra, A.F., Toga, A.W., 2000. Mapping morphology of the corpus callosum in schizophrenia. Cereb. Cortex 10, 40–49.

Oh, J.S., Park, K.S., Song, I.C., Kim, S.J., Hwang, J., Chung, A., Lyoo, I.K., 2005. Fractional anisotropy-based divisions of the midsagittal corpus callosum. NeuroReport 16, 317–320.

Park, H.-J., Kubicki, M., Shenton, M.E., Guimond, A., McCarley, R.W., Maier, S.E., Kikinis, R., Jolesz, F.A., Westin, C.F., 2003. Spatial normalization of diffusion tensor MRI using multiple channels. NeuroImage 20, 1995–2009.

Park, H.J., Lee, J.D., Chun, J.W., Seok, J.H., Yun, M., Oh, M.K., Kim, J.J., 2006. Cortical surface-based analysis of 18F-FDG PET: measured metabolic abnormalities in schizophrenia are affected by cortical structural abnormalities. NeuroImage 31, 1434–1444.

Peters, M., Oeltze, S., Seminowicz, D., Steinmetz, H., Koeneke, S., Jancke, L., 2002. Division of the corpus callosum. Brain Cogn. 50, 62–72.

Shin, Y.-W., Kim, D.J., Ha, T.H., Park, H.J., Moon, W.J., Chung, E.C., Lee, J.M., Kim, I.Y., Kim, S.I., Kwon, J.S., 2005. Sex differences in the corpus callosum: diffusion tensor imaging study. NeuroReport 16, 795–798.

Smith, S.M., Jenkinson, M., Johansen-Berg, H., Rueckert, D., Nichols, T.E., Mackay, C.E., Watkins, K.E., Ciccarelli, O., Cader, M.Z., Matthews, P.M., Behrens, T.E., 2006. Tract-based spatial statistics: voxelwise analysis of multi-subject diffusion data. NeuroImage 31, 1487–1505.

Sullivan, E.V., Rosenbloom, M.J., Desmond, J.E., Pfefferbaum, A., 2001. Sex differences in corpus callosum size: relationship to age and intracranial size. Neurobiol. Aging 22, 603–611.

Thottakara, P., Lazar, M., Johnson, S.C., Alexander, A.L., 2006. Application of Brodmann's area templates for ROI selection in white matter tractography studies. NeuroImage 29, 868–878.

Tuch, D.S., 2004. Q-ball imaging. Magn. Reson. Med. 52, 1358–1372.

Vikingstad, E.M., George, K.P., Johnson, A.F., Cao, Y., 2000. Cortical language lateralization in right handed normal subjects using functional magnetic resonance imaging. J. Neurol. Sci. 175, 17–27.

Witelson, S.F., 1989. Hand and sex differences in the isthmus and genu of the human corpus callosum: a postmortem morphological study. Brain 112, 799–835.

Witelson, S.F., Goldsmith, C.H., 1991. The relationship of hand preference to anatomy of the corpus callosum in men. Brain Res. 545, 175–182.

Wu, J.C., Buchsbaum, M.S., Johnson, J.C., Hershey, T.G., Wagner, E.A., Teng, C., Lottenberg, S., 1993. Magnetic resonance and positron emission tomography imaging of the corpus callosum: size, shape and metabolic rate in unipolar depression. J. Affect. Disord. 28, 15–25.

Xu, D., Mori, S., Shen, D., van Zijl, P.C., Davatzikos, C., 2003. Spatial normalization of diffusion tensor fields. Magn. Reson. Med. 50, 175–182.